Journal of Environmental Management 240 (2019) 160–167

Contents lists available at ScienceDirect

Journal of Environmental Management

journal homepage: www.elsevier.com/locate/jenvman

Research article

Impacts of iron oxide and titanium dioxide nanoparticles on biogas production: Hydrogen sulfide mitigation, process stability, and prospective challenges

Mohamed Farghali[a,b], Fetra J. Andriamanohiarisoamanana[a], Moustafa M. Ahmed[b], Saber Kotb[b], Takaki Yamashiro[a], Masahiro Iwasaki[a], Kazutaka Umetsu[a,*]

[a] Graduate School of Animal and Food Hygiene, Obihiro University of Agriculture and Veterinary Medicine, Obihiro, Hokkaido, 080-8555, Japan
[b] Department of Animal Hygiene, Faculty of Veterinary Medicine, Assiut University, 71526, Egypt

ARTICLE INFO

Keywords:
Metal oxide nanoparticles
Hydrogen sulfide
Biogas
Methane
Anaerobic digestion
Manure treatment

ABSTRACT

Anaerobic digestion for biogas production is one of the most used technology for bioenergy. However, the adoption of nanoparticles still needs further studies. Therefore, this study was designed to examine the effect of metal oxide nanoparticles (MONPs) at four different concentrations in two different combinations, 20 (R1) and 100 (R2) mg/L for Fe_2O_3, 100 (R3) and 500 (R4) mg/L for TiO_2, and a mixture of Fe_2O_3 and TiO_2 at rates of 20, 500 (R5) and 100, and 500 (R6), on hydrogen sulfide (H_2S) mitigation, biogas, and methane (CH_4) yield during the anaerobic digestion of cattle manure (CM) using an anaerobic batch system. The results showed that H_2S production was 2.13, 2.38, 2.37, 2.51, 2.64, and 2.17 times lower than that of the control (R0), respectively, when the CM was treated by the aforementioned MONPs. Additionally, biogas and CH_4 production were 1.09 and 1.105, 1.15 and 1.191, 1.07 and 1.097, 1.17 and 1.213, 1.10 and 1.133, and 1.13 and 1.15 times higher than those of R0 when R1, R2, R3, R4, R5, and R6 were supplemented with MONPs, respectively. The highest specific production of biogas and CH_4 was 336.25 and 192.31 mL/gVS, respectively, which was achieved by R4 supplemented with 500 mg/L TiO_2 NPs, while the corresponding values in the case of R0 were 286.38 and 158.55 mL/gVS.

1. Introduction

The production of economic and environmentally sustainable renewable energy sources is a core area of contemporary research and industry. The anaerobic digestion (AD) of cattle manure (CM) has enticed considerable attention within the scientific community, because of improving in hygienic standards of digested nutrients and promoting renewable alternatives through the production of methane (CH_4) rich biogas (Zhang et al., 2018). Biogas usually consists of CH_4 (40–75%) and CO_2 (25–60%), with trace amounts of other impurities, including hydrogen sulfide (H_2S) (Kadam and Panwar, 2017). The concentration of H_2S in biogas ranges from 50 to 10,000 ppm, depending on the composition of the feed material to be digested (Muñoz et al., 2015; Pipatmanomai et al., 2009). Elevated levels of H_2S in biogas cause several problems, for example, H_2S significantly reduces the volume and potential uses of biogas as it is highly corrosive to the biogas purification instruments (Charles et al., 2006; Zhou et al., 2016). Additionally, it is highly poisonous and has led to the death of many people (Andriamanohiarisoamanana et al., 2015). Therefore, the presence of H_2S in biogas is one of the main obstacles to the successful implementation of AD and must be minimized to a level that can be tolerated by equipment, for example, between 200 and 500 mg/L to protect downstream biogas equipment and internal combustion engines (Lupitskyy et al., 2018).

In practice, some popular biological (such as biofilters) and chemical (such as sodium hydroxide scrubbing and iron oxide pellets) techniques have been applied to control H_2S (Bioenergy, 1999). However, post-H_2S removal techniques are costly, require the handling of chemicals, and lack long-term stability, which greatly limits their commercialization (Blazy et al., 2014). Therefore, it is essential to remove H_2S during the AD process by direct mixing the feed materials to be digested with additives and then analyze the possible regulatory pathway of the entire process. In this context, it is assumed that the addition of trace minerals to feed the stream improves AD by enhancing the bacterial action that increases biogas generation. In AD, trace minerals supplements serve as electron donors as they promote the total

* Corresponding author.
E-mail address: umetsu@obihiro.ac.jp (K. Umetsu).

https://doi.org/10.1016/j.jenvman.2019.03.089
Received 24 January 2019; Received in revised form 6 March 2019; Accepted 18 March 2019

hydrogen uptake, release ions that contribute to the production of key essential enzymes required by AD microflora, and eventually enhance the number of methanogens (Liu et al., 2015; Qiang et al., 2013). Admittedly, iron salt and scrap iron have been used to improve the stability of AD and increase methane production (Zhang and Jahng, 2012; Zhang et al., 2014b) or mitigate H_2S production (Andriamanohiarisoamanana et al., 2018). However, there is little to no literature reporting the effects of nanoscale metals on the AD of CM.

Nanotechnology is an emerging, novel branch of science, and is linked with materials smaller than 100 nm (Nel et al., 2006). Metal oxide nanoparticles (MONPs) are a fundamental nano-scale material that could revolutionize current diagnostic and therapeutic techniques due to their unique features, including their superparamagnetic performance, high surface area to volume ratio, and easy separation using an external magnetic force (Sun et al., 2008). In this regard, nano-iron has been reported to successfully enhance the presence of methanogens in digested sludge. In the AD of cattle slurry, Abdelsalam et al. (2016) found that the biogas yield was 1.7 times higher than that of the control when the feed was supplemented with iron oxide (Fe_3O_4 NPs) at a dosage of 20 mg/L. Additionally, during a study on the AD of activated sludge, Wang et al. (2016b) found that supplementation with Fe_2O_3 NPs at 100 mg/g total suspended solids (TSS) improved the CH_4 yield to 117%. Casals et al. (2014) also observed the benefits of the unique characteristics of Fe_3O_4 NPs, which slowly dissolved to supply microorganisms in the AD of waste at a moderate temperature (37 °C) for 60 days. An Fe_3O_4 NPs (7 nm) dosage of 100 mg/L^{-1} enhanced the biogas and CH_4 yields by 180% and 234%, respectively, which was the greatest improvement to biogas production, according to the author's findings. However, improved H_2S removal may be attributed to the interaction between the Fe (II)/Fe (III) oxide layer formed on the NP surface and sulfides (Su et al., 2013). Therefore, the addition of Fe_2O_3 NPs to biodigesters could improve methane generation and stabilize the AD process.

Titanium dioxide (TiO_2) NPs is the second most extensively applied nanomaterial after iron worldwide. Approximately 50,400 tons of TiO_2 NPs were manufactured in 2010, accounting for 0.7% of the general TiO_2 manufacture. Production is set to expand to 201,500 tons by 2015 (Future-markets, 2011). TiO_2 NPs are well recognized as having long-term stability and strong photocatalytic activity, and serve as a powerful oxidative stress inducer that allows the generation of reactive oxygen species (ROS) under specific conditions, such as a certain light wavelength (Kubo et al., 2005; Rincón and Pulgarin, 2003). Hence, they are used as a broad germicidal agent to a wide range of bacteria, including both Gram-positive and Gram-negative species (Adams et al., 2006). This germicidal action of TiO_2 NPs may be the reason for their limited use in the AD process. However, some researchers (Chen et al., 2014; Gonzalez-Estrella et al., 2013; Mu et al., 2011) reported that the viability of anaerobic microbial communities and activities of essential enzymes related to CH_4 production, such as acetate kinase, protease, and coenzyme F420, is unaffected by the long-term presence of TiO_2 NPs at up to 150 mg/g TSS. Moreover, the aforementioned authors documented that the effect of TiO_2 on the generation of CH_4 was not remarkably impacted due to the insolubility of TiO_2 NPs. In contrast, Cervantes-Aviles et al. (2018) found that CH_4 production increased by 14.9% after adding TiO_2 NPs to wastewater and waste sludge in anaerobic digesters. Furthermore, 8% of the TiO_2 NPs remained in the treated effluent, while 92% was removed by the anaerobic sludge. Furthermore, Garcia et al. (2012) observed a 10% improvement in the biogas yield after the addition of TiO_2 NPs in a thermophilic anaerobic experiment. TiO_2 NPs could also be suitable for H_2S control due to their superior catalytic features, such as the active sites on their surfaces and their ability to adsorb and interact with H_2S/SO_2 and form a strong, irreversible Ti−SH bond (Yanxin et al., 1999).

Some studies analyzed the effects of Fe_2O_3 and TiO_2 NPs on biogas and CH_4 production. However, the application of MONPs in cattle manure that has a high concentration of biomass, dense microbial aggregate structure, and excellent sedimentation capacity, is expected to result in a different response of the NPs towards the digestate environment and may boost bacterial activity and digestion stability. Therefore, this study is designed to be the first of its kind to achieve the following objectives: to determine the effects of Fe_2O_3 and TiO_2 NPs on CH_4 generation during the AD of cow manure; to discover the novel effects of various NPs on the removal of H_2S from the AD system; and to explore the combined action of using the two nanoparticles on CH_4 and H_2S in a batch system.

2. Materials and methods

2.1. Materials

Commercial iron oxide (Fe_2O_3, 20–40-nm sized particles) and titanium dioxide (TiO_2, 25 nm) were purchased from Wako Chemical Industries Co., Ltd., (Japan). The purity of both MONPs exceeded 99%, and they were both in powder form. Fresh dairy cattle manure (CM) was randomly gathered from the concrete floor of a free stall barn in Obihiro University (OUAVM), Japan, and used as the substrate in this study. The digested slurry inoculum was assembled from mesophilic active biogas plants in Obihiro, Hokkaido, Japan. The CM and inoculum were distributed to the biodigesters at a ratio of 1:1, based on their VS contents. Before seeding, the inoculum was placed in a thermo-controlled water bath at a mesophilic temperature (38 °C) for two days to reduce the contribution of the remaining organic matter in the inoculum. Details of the chemical features of the raw CM and inoculum are presented in Table 1.

2.2. Experimental setup

In this study, the influence of adding different types, concentrations, and combinations of metal oxide nanoparticles on H_2S removal, and biogas and CH_4 generation was investigated by conducting a series of laboratory batch experiments, in addition to their impact on digestion performance and stability. Based on these objectives, 1-L polypropylene biodigesters with a working volume of 600 mL were used in this experiment.

The series of batch digesters was filled with a calculated quantity of substrate and inoculum. Six MONP treatments (R1 to R6) were added directly to the biodigesters, as follows: R1 to R4 supplemented the substrates with 20 and 100 mg/L substrate of Fe_2O_3, and 100 and 500 mg/L substrate of TiO_2 respectively, while the last two treatments, i.e., R5 and R6, were a mixture of both Fe_2O_3 and TiO_2 at proportions of 20 Fe_2O_3 + 500 TiO_2 and 100 Fe_2O_3 + 500 TiO_2, respectively. The concentrations of Fe_2O_3 (20 and 100 mg/L) were selected based on the findings of Abdelsalam et al. (2017, 2016) and Casals et al. (2014). Few studies have considered the impact of TiO_2 on the AD process, but some researchers mentioned that it is safe at concentrations below 150 mg· (g TSS) $-^1$ (Chen et al., 2014; Garcia et al., 2012). However, other researchers observed no inhibitory effect on AD at concentrations up to

Table 1
Chemical characteristics of the inoculum and raw CM.

Digester	pH	TS %	VS %	VS/TS	ASH %[a]
Inoculum	7.67	8.03	5.76	0.717	2.27
R0	7.11	8.88	6.97	0.785	1.92
R1	7.09	8.83	6.95	0.787	1.88
R2	7.11	9.47	7.55	0.798	1.91
R3	7.06	9.16	7.26	0.793	1.89
R4	7.11	9.46	7.47	0.790	1.96
R5	7.14	9.04	7.14	0.789	1.91
R6	7.09	9.19	7.30	0.794	1.86
Cattle manure	6.36	12.45	10.82	0.869	1.63

[a] TS: Total solids, VS: Volatile solids.

Table 2
Design of batch experiment.

Digester	Fe_2O_3 NPs		TiO_2 NPs		Quantity of inoculum (g)	Quantity of CM (g)	Quantity of water (g)
	mg added	mg/L	mg added	mg/L			
R0	0	0	0	0	375	200	25
R1	4	20	0	0	375	200	25
R2	20	100	0	0	375	200	25
R3	0	0	20	100	375	200	25
R4	0	0	100	500	375	200	25
R5	4	20	100	500	375	200	25
R6	100	500	100	500	375	200	25

Table 3
Individual volatile fatty acid contents before and after the AD process.

Digester	Before AD					After AD[a]			
	Formic acid (mg/L)	Acetic acid (mg/L)	Propionic acid (mg/L)	Butyric acid (mg/L)	TVFA (mg/L)	Formic acid (mg/L)	Acetic acid (mg/L)	TVFA (mg/L)	TVFA removal %
R0	1.974	248.780	83.554	29.973	364.281	0	10.005	10.005	97.25
R1	2.484	235.947	76.899	29.246	344.576	1.997	10.058	12.054	96.50
R2	2.749	231.703	76.280	27.863	338.595	0	10.787	10.787	96.81
R3	2.207	235.641	78.549	29.687	346.084	0	10.041	10.041	97.10
R4	3.073	250.364	87.344	29.274	370.055	0	9.846	9.846	97.34
R5	0.000	253.618	90.132	35.676	379.426	0	10.000	10.000	97.36
R6	0.000	250.841	85.845	34.082	370.768	0	8.597	8.597	97.68

[a] The values of propionic acid and butyric acid for "After AD" were zero.

1500 mg/L (Cervantes-Aviles et al., 2018; Gonzalez-Estrella et al., 2013). Therefore, we employed TiO_2 NP concentrations of 100 and 500 mg/L substrate. The final group (R0) was the control (fed only with the CM and inoculum, with no MONPs). The full details of the experimental design are presented in Table 2. Finally, 25 g of water was added to each biodigester to meet the 600 mL working volume. Each group from R0 to R6 was tested in triplicate, in addition to blank digesters (Inoculum only). All digesters were fully closed and placed in a thermally controlled water bath at 38 °C with a hydraulic retention time (HRT) of 30 days. During the 30-day incubation period, all biodigesters were mixed manually for 1 min daily, before the gas volume was measured to reduce the stratification of the digestate as much as possible (Zhang et al., 2014a).

2.3. Analysis of different parameters

The hydrogen sulfide (H_2S) content of the gas was measured daily for the first 10 days, and every two to three days thereafter until day 30. The H_2S was measured from the headspace of the digesters using a manual gas pump (Model AP-1, Komyo Kitagawa, Japan) equipped with two different fast-measuring tube detectors (Gastec Co., Japan). Gastec No. 4M and 4H were used to measure the H_2S concentrations by pulling the gas pump at 100%. All H_2S measurements were recorded in ppm (Andriamanohiarisoamanana et al., 2018, 2017b).

Two-liter Tedlar® gas-bags were used to collect the biogas, and its volume was quantified using a wet-drum gas meter. The gas contents (CH_4) were assessed using a GC-14A gas chromatograph (GC, Shimadzu, Japan) equipped with a thermal column detector and Porapak Q packing. The operation temperature of the column, injector port, and detector were 150, 220, and 220 °C, respectively. Argon was used as the carrier gas at an influx of 50 mL/min. The gas composition and volume were measured daily until day 10, and then every 2–5 days, depending on its volume. The volatile fatty acids (VFAs), total solids (TSs), pH, and volatile solids (VSs) in each biodigester were assessed before and after the batch test. VFAs consisting of acetic (CH_3COOH), formic (HCOOH), butyric (C_3H_7COOH), and propionic (CH_3CH_2COOH) acids were analyzed using high-performance liquid chromatography (HPLC, LC-10 AD, Shimadzu, Japan) with a SCR-102H Shim-Pack column. The full procedure was explained in detail by Lateef et al. (2014). Standard methods were followed to calculate the TS and VS contents (APHA, 2005). Briefly, TSs were measured by drying the samples at 105 °C for 24 h, and the solid contents were determined from the difference between the samples' weights before and after drying. The VS content was calculated from the loss on ignition after ashing the dried residue at 550 °C for 4 h. Finally, the pH values of the digestates were detected using a Horiba pH meter (model D-55).

2.4. Data analysis and calculations

The biogas and methane levels generated from the inoculum (Blank) were subtracted from those generated from the sample assays. The cumulative biogas (CBY) and methane (CMY) yields of each treatment (from R0 to R6) were calculated by dividing the CBY or CMY generated during the 30-day period by the initial total mass of VS in each digester (Zhang et al., 2014a), and the results were expressed as CBY or CMY per gVS added.

The H_2S reduction efficiency of the treated digesters was calculated using Eq. (1).

$$RE\% = \{1 - \frac{[H\ td]}{[H\ cd]}\}. 100 \quad (1)$$

where RE% is the H_2S reduction efficiency, H td is the H_2S content of the treatment digester, and H cd is the H_2S content of the control digester.

VS removal % was calculated based on the total mass removal from the tested bio-digesters after subtracting the VS of the blank inoculum digesters, as illustrated in Eq. (2) according to Andriamanohiarisoamanana et al. (2017a).

$$VSs = VSr + \frac{[VS\ inoc.\ ad]}{[VS\ sub.\ ad]}. (VSr - VSi) \quad (2)$$

where VSs (%) is the VS reduction of the substrate alone, VSr (%) is the total VS reduction of the substrate and inoculum, VSinoc.ad is the VS of the inoculum added (g/kg), VSsub.ad is the VS of cattle manure added

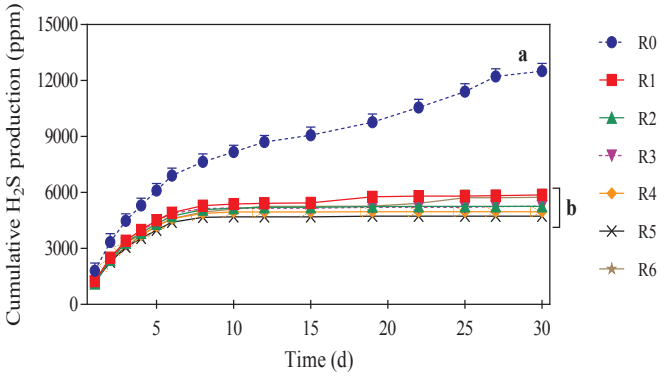

Fig. 1. Cumulative H_2S yield during the 30-day experimental period.

(g/kg), and VSi (%) is the VS reduction of the inoculum alone.

The data were statistically analyzed performed at a probability level of 0.05 using SPSS version 18 (PASW Statistics for Windows, Chicago, USA). The effects of Fe_2O_3 and TiO_2 NPs, and their combinations were assessed by one-way ANOVA followed by a Tukey post-hoc test at $P < 0.05$. The data are expressed as average + standard error (SEM). All figures are presented as parameter values plus SEM and were prepared using GraphPad Prism version 7 for Windows (GraphPad Software, La Jolla CA, USA).

3. Results and discussions

3.1. Impact of MONPs on hydrogen sulfide concentration

The results of cumulative H_2S production throughout the experimental period indicated a significant reduction in H_2S production ($P < 0.05$) by the addition of MONPs, as illustrated in Fig. 1. In particular, the cumulative H_2S concentrations of R1, R2, R3, R4, R5, and R6 were 5863.33, 5250.00, 5263.33, 4972.50, 4733.33, and 5747.50 ppm, respectively, while that of the control was 12480.00 ppm. The peak H_2S values were recorded in the first 3 days for all biodigesters, and the highest was observed in R0 (1780 ppm). Thereafter, the H_2S reduced in all digesters until day 30, as shown in Fig. 2. On average, in the digesters treated with MONPs, H_2S decreased by 33.03, 35.81, 35.08, 35.90, 41.55 and 36.83%, respectively, from day one to nine. Thereafter, there was a sharp decrease in H_2S, with average reductions of 88.29, 96.44, 97.47, 98.10, 98.77, and 83.82% for the aforementioned MONP-treated digesters, respectively (Fig. 3).

The bio-availability of organic matter and sulfate in the anaerobic digestate stimulates the growth of *sulfate-reducing bacteria* (SRB), which reduce sulfur to sulfide as a terminal electron receiver from a wide range of elements, such as H_2, ethanol, formate, succinate, pyruvate, and lactate (Muyzer and Stams, 2008), and produce H_2S as the final product gas. In this context, MONPs effectively mitigated the H_2S emissions in all treated biodigesters by killing the SRB, directly

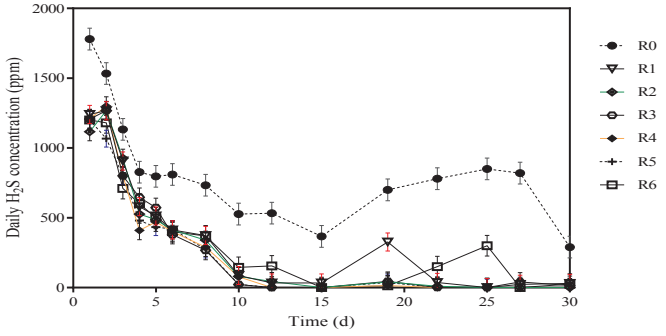

Fig. 2. Specific H_2S production during the 30-day experimental period.

absorbing the sulfur in the digestate, or altering the contaminating elements through a specific biochemical process (Ševců et al., 2011; Yang et al., 2013). The toxicity mechanisms of metallic NPs may comprise corruption of the cell membrane permeability, enzyme inactivation and DNA disruption caused by released metal ions, and apoptosis combined with the generation of intracellular reactive oxygen species (ROS) (Kim et al., 2010; Marsalek et al., 2012; Yang et al., 2013). However, these mechanisms were excluded as our experiments were conducted under dark and anaerobic conditions, and oxidative stress caused by ROS is not possible. In addition, the photocatalytic abilities of metals NPs are negligible (Ambuchi et al., 2017). Moreover, the amounts of MONPs used in this study were far lower than the inhibition concentration of iron NPs (10 g/L) on SRB as documented by (Kumar et al., 2014). Additionally, there was no significant difference between the pH of R0 and MONPs test digesters as given in Table 4, indicating the pH of digestate after the AD progress was favorable for anaerobic microbial growth, including SRB, and thus, H_2S in the digestate was supposedly similar for all digesters under study including R0. Therefore, the possible reason for the mitigation of H_2S emissions in this study is the precipitation of metal sulfides, such as ferrous sulfide (FeS), which is consistent with the results mentioned in the literature (Andriamanohiarisoamanana et al., 2018; Sarker et al., 2018). Finally, H_2S may predominantly be absorbed on the surface TiO_2 in the form of SO_2/SO_3, forming irreversible Ti−S bonds, which was explained by Yanxin et al. (1999).

The reason for the lower efficiency of MONPs in R6 than those in R5 during AD may be explained as follows: first, the ratio of iron and titanium NPs in R6 may have increased the rates of the aggregation and agglomeration, and increased the possibility of collision (Casals et al., 2012; Gonzalez-Estrella et al., 2013). This may have resulted in the creation of different-sized particles, different surfaces, and reduced the mobility of NPs that are different from the initial NPs and re-aggregate rapidly upon resuspension (Casals et al., 2012). We agitated the contents of the digesters once daily. Accordingly, the interactions between MONPs and sulfur/sulfate decreases, allowed the SRB bacteria to utilize more sulfate, and result in the production of H_2S in R6. The rate of aggregation in R6 is not excessively large as the combined MONPs could significantly reduce the content of H_2S by 53.95% from that of R0 (Figs. 1 and 4). Secondly, the ratio of the two MONPs in R6 led to the formation of a mixed oxide, pseudobrookite, which causes a competing electron interaction between metal structures, resulting in the dispersion of the Ti^{3+}/Ti^{4+} and Fe^{2+}/Fe^{3+} redox pairs on the NPs' surfaces (Wang and Ro, 2007). Nonetheless, a synergistic effect was achieved by combining Fe_2O_3 with TiO_2 NPs in R5. In addition, R5 exhibited no or little aggregation between the two MONPs, allowing better contact and more interactions between the NPs and the sulfate, resulting in the highest H_2S removal efficiency of 62.07%, as indicated in Fig. 4.

3.2. Impact of MONPs on biogas and CH_4 production

In this study, it was anticipated that the application of MONPs in the AD of CM would either inhibit or enhance substrate degradation and bio-methanation. This hypothesis was confirmed by examining the responses of CM to nano-Fe_2O_3 and nano-TiO_2, either individually or in combinations.

3.2.1. Effects of MONP exposure on biogas production

Biogas production was improved when the CM substrates were exposed to MONPs at all concentrations and combinations in comparison to the control. Fig. 5 illustrates the cumulative impacts of different Fe_2O_3 and TiO_2 NP dosages on biogas yields during the AD of CM, which were 310.87, 328.64, 306.96, 336.25, 315.22, and 323.86 mL/gVS for R1, R2, R3, R4, R5, and R6, respectively, while that of R0 was 286.38 mL/gVS. The specific daily biogas production curve presented in Fig. 6 indicates that the production of biogas began on the first day and increased until day 13. Thereafter, there was an abrupt decrease in

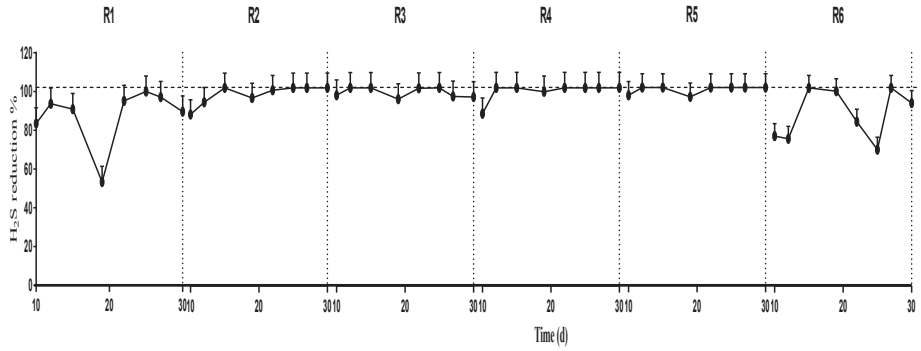

Fig. 3. H_2S removal efficiency from day 10 until the end of the experiment.

Table 4
Chemical characteristics of the digestate and Vs removal after the AD process.

Digester	pH	TS%	VS%	VS removal of substrate (%)
Inoculum	7.85	7.92	5.60	
R0	7.48	6.67	4.75	47.38
R1	7.48	6.52	4.66	49.00
R2	7.49	6.66	4.79	54.56
R3	7.46	6.71	4.83	49.78
R4	7.45	6.35	4.51	59.16
R5	7.52	6.42	4.54	54.16
R6	7.48	6.52	4.64	54.26

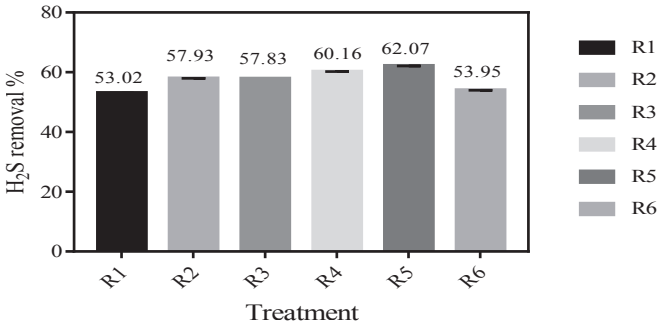

Fig. 4. Removal % of H_2S by MONPs during the batch experiment.

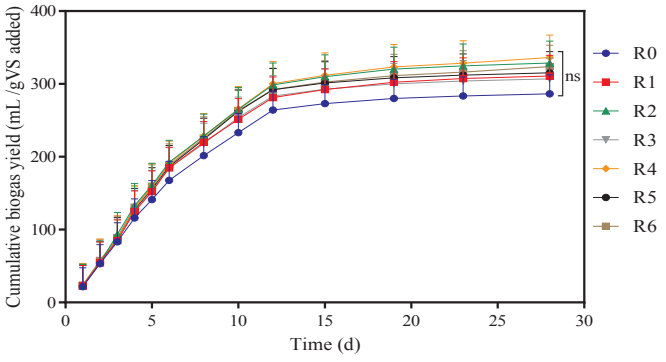

Fig. 5. Cumulative biogas yield/gVS of cattle manure.

biogas production until the end of the experimental period. Furthermore, all MONP additives reduced the time required to reach the highest biogas yields compared with that of control; the maximum daily biogas yield was 33.83 mL/gVS, which was achieved on day eight for the control, while those of R1 to R6 were 39.71, 39.51, 39.57, 41.17, 40.25, and 41.43 mL/gVS, respectively, which were achieved on day four.

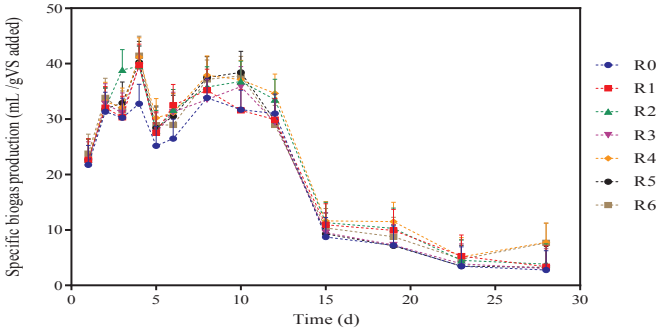

Fig. 6. Specific biogas production/gVS of cattle manure.

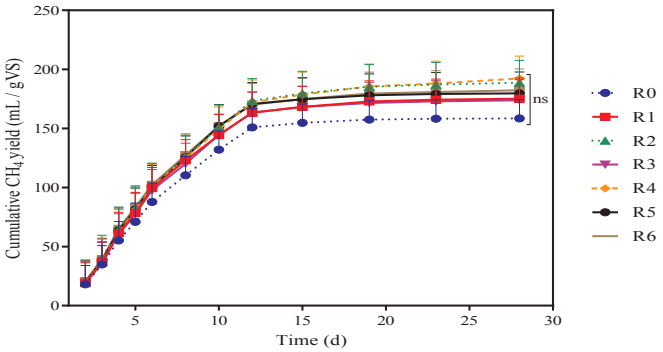

Fig. 7. Cumulative methane yield/gVS of cattle manure.

3.2.2. *Effects of MONP exposure on CH_4 production*

The cumulative CH_4 yields and their flow rates when the substrates were exposed to MONPs in R1 to R6 for 30 days were 175.16, 188.76, 173.85, 192.31, 179.68, and 182.29 mL/gVS, respectively, as shown in Fig. 7, while R0 yielded 158.55 mL CH_4 per gVS. In particular, as shown in Fig. 7, CH_4 production increased when the concentrations of MONPs increased, as the CH_4 yield was 1.11 and 1.08 times higher in R4 and R2 than those in R3 and R1, respectively. Additionally, the exposure of the substrates to a mixture of MONPs in R6 resulted in a CH_4 yield that was 1.01 times higher than that in R5.

Fig. 8 shows the specific CH_4 production trend over the 30 days of the experiment. The specific CH_4 generation began from the first day and fluctuated. Furthermore, adding MONPs to the biodigesters appeared to enhance the methanogenic bacteria and stabilize the AD process throughout the 30 days of the experiment, particularly during the final stage (last 15 days). Ultimately, the CH_4 concentration increased in all NP-treated digesters; those of R4 and R2 were 1.102 and 1.097 times higher than that of the control, respectively, as illustrated in Fig. 9, and this corresponds to the increase in the biogas and CH_4 yields of these digesters.

The addition of nano-Fe_2O_3 to the substrates at a dosage of 100 mg/

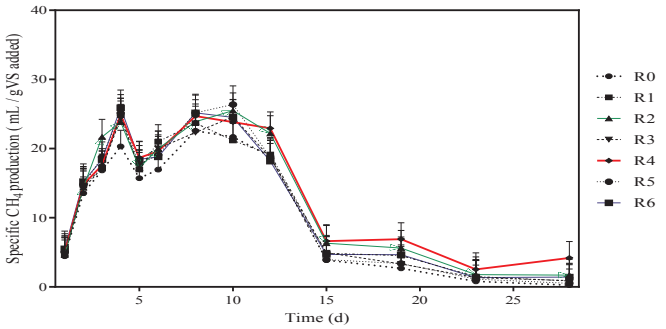

Fig. 8. Specific CH_4 production/gVS of cattle manure.

L resulted in biogas and CH_4 yields that were 1.15 and 1.19 times higher, respectively, as shown in Figs. 5 and 7, which is comparable with the results of Wang et al. (2016b), who found that the supplementation of a substrate with 100 mg/g TSS Fe_2O_3 of NPs promoted the CH_4 yield to 117% of that of the control group. However, our results are lower than those of Abdelsalam et al. (2017, 2016), who used 20 mg/L of iron oxide NPs and observed biogas and CH_4 yields that were 1.7 and almost 2 times higher than those of the untreated control, respectively. The differences in the results of these authors may be attributed to differences in the sizes of NPs, substrates, and experimental conditions. Abdelsalam et al. (2017, 2016) continually mixed the slurry using a fixed motor for 1 min every 1 h. This ensures continuous suspension of the MONPs and increased their exposer to anaerobic bacteria. However, using 500 mg/L of nano-TiO_2 resulted in biogas and CH_4 yields that were 1.17 and 1.213 times higher than those of the control, respectively. This result is extremely motivating and higher than those of the previous reports by Garcia et al. (2012) and Cervantes-Aviles et al. (2018), who observed increases in biogas yields of only 10 and 14.9%, respectively, after adding TiO_2 NPs to anaerobic digesters. However, Li et al. (2017) noticed adding 5 mg/L of nano-TiO_2 to digesters reduced the CH_4 and biogas yields by 14.01 and 30.70%, respectively.

The improved biogas and CH_4 production efficiencies caused by Fe_2O_3 NPs can be attributed to several reasons. First, the release of $Fe^{+2/+3}$ from the Fe_2O_3 NPs provided iron ions in the biodigester and effectively promoted the activity of methanogenic archaea, increasing the CH_4 content (Abdelsalam et al., 2017; Mu and Chen, 2011). Second, the Fe_2O_3 NPs may stimulate the production of extracellular polymeric substances by anaerobic bacteria, which provide cell protection against microbial cytotoxicity (Ambuchi et al., 2017). Finally, the enhanced influence of both MONPs can be attributed to the uptake of NPs by methanogens, which used the metabolic intermediates and primary enzyme biosynthesis involved in sludge hydrolysis, acidification, acetification, and methanation, which efficiently converted the anaerobic substrates irreversibly to CH_4 (Mu et al., 2011; Yang et al., 2013). According to some authors (Cervantes-Aviles et al., 2018; Wang et al., 2016a), nano-TiO_2 can efficiently export extracellular electrons from inside the cell to extracellular ions through extracellular electron transfer (EET), which enhanced the production of CH_4 by the anaerobic biodigesters in our experiments. The results also indicated higher biogas and CH_4 production in a dose-response manner by both the individual and mixtures of MONPs, which can be further explained by the findings of Mu and Chen (2011), who noticed that the hydrolysis of soluble proteins and the electron-exporting ability of electron donors in methanogenic Archaea expressed by coenzyme F420 are controlled by higher concentrations of nanoparticles (i.e., they are nanoparticle dosage-dependent). The higher CH_4 production with individual MONPs than their mixtures in R6 and R5 can be attributed to their aggregation and cluster formation caused by their combination, which reduces the physical contact between bacteria and the NPs' surfaces (Wang et al., 2016a), reducing both the EET and uptake of NPs by bacteria, thereby reducing the activity of methanogens.

3.3. Impact of MONP dosages on process stability, VFA, and VS removal

In general, the total volatile fatty acid (TVFA) contents did not vary significantly after treatment with both MONPs from that of the control. As shown in Table 3, the TVFA ranged between 338.595 and 379.426 mgL^{-1}, indicating that microbial activity had harmonized (Ahring, 1995). Additionally, the obtained pH values varied between 7.45 and 7.52 in the treated digesters, while that of the control was 7.48, as shown in Table 4. Accordingly, the AD process appeared to operate in a stable manner with a healthy set of pH values.

It should be noted that all MONP-treated digesters produced acceptable levels of CH_4 that exceeded those of the control (55.97–59.14% compared to 53.68% for the control) during the 30-day experimental period, indicating good utilization of acetic, propionic, formic, and butyric acid. Additionally, the MONPs accelerated the transfer of electrons from acetogens as an energy source for the methanogens, resulting in higher conversion of VFAs to CH_4 and CO_2 (Noonari et al., 2018). In this context, the higher amount of acetic acid in R1, R2, and R3 than those in R4, R5, R6, and R0, as illustrated in Table 3, can be interpreted as follows: acetogens decompose the main products of the hydrolysis of organic substances, i.e., fatty acids and alcohols to acetic acid, CO_2, and H_2, which are utilized by methanogenic Archaea to form biogas (typically 60% CH_4, 38% CO_2 and 2% trace gases). CH_4 is mostly produced through the decomposition of acetate by acetoclastic methanogens and the utilization of H_2/CO_2 by hydrogen-utilizing methanogens (Sarker et al., 2018). Between these two CH_4 production pathways, two-thirds of the CH_4 gas are produced during the anaerobic conversion of acetate by microbes, and

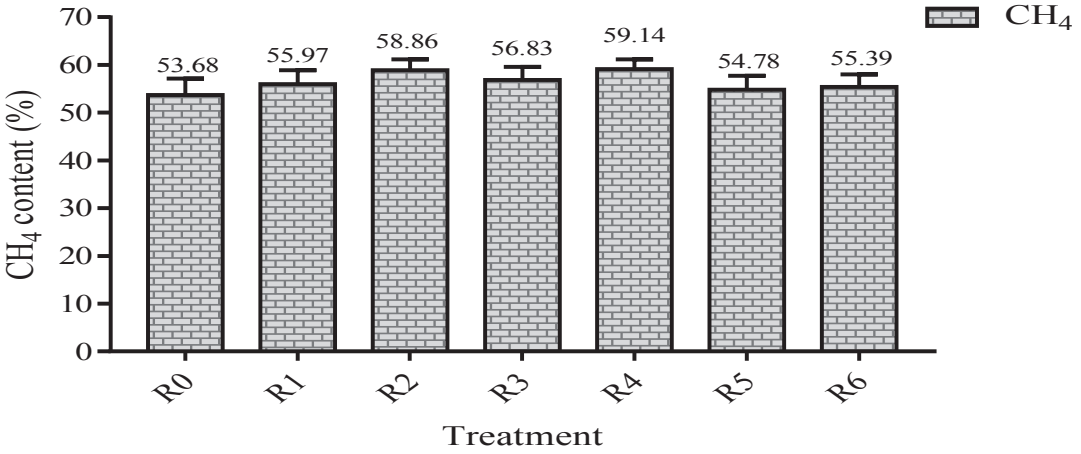

Fig. 9. CH_4 concentrations in the different cattle manure treatments.

approximately one-third is produced from H_2/CO_2 reduction (Bajpai, 2017). Therefore, the MONPs promoted the transformation of H_2/CO_2 to CH_4, which may be the reason for the increased CH_4 production in R1, R2, and R3, despite their higher acetic acid contents. These findings were comparable to those of Sarker et al. (2018), who found that the highest gas emissions were produced by anaerobic digesters with higher acetic acid contents, indicating that the gas was likely to be produced by H_2/CO_2 reduction.

Table 4 shows the chemical characteristics of CM, i.e., the percentages of TS, VS, and VS removal, after the 30-day batch experiment. The VS reductions in R1, R2, R3, R4, R5, and R6 were 1.03, 1.15, 1.05, 1.25, 1.14, and 1.15 times higher than that in R0, respectively. The changes in the VS contents with the addition of MONPs indicated enhanced organic matter degradation, which contributed to the variations in the CH_4 yields as described in Table 4 and Fig. 7. The highest VS decomposition was observed when the substrate was treated with 500 mg/L of TiO_2 NPs, followed by that with 100 mg/L Fe_2O_3 (59.16 and 54.56% removal rates, respectively). These results agree with the findings of Abdelsalam et al. (2017), who also observed increases in the biogas and CH_4 yields with increased addition of metal NPs to cattle slurry biodigesters.

4. Challenges and future studies

The results of this experiment illustrate that the anaerobic bacterial and Archaeal activities, as well as the degradation of organic matter, are promoted by the addition of different dosages of MONPs. However, such an application method might cause some environmental concern regarding their toxicity towards the bacteria in manure, soil, and neighboring ecosystems, rather than their accumulative residual toxicity in soils. The findings of many studies indicate the beneficial effects of using iron oxide NPs in soils for crop protection, remediating organic soil contaminants, and nano-fertilization (Liu and Lal, 2015; Zhang et al., 2014a). Additionally, the toxic effects of TiO_2 NPs in soils were discussed by many researchers (Lyu et al., 2017; Skocaj et al., 2011) who found that they are advantageous supplements for plant growth, and demonstrated their role in the improvement of nitrogen photosynthesis, nutrient uptake and metabolism, and crop quantity and quality. However, to increase caution and avoid any environmental consequences, the indirect application of NPs in manure biodigester systems, such as their entrapment in porous media and the preparation of biofilters coated with them, could be assessed in further studies. This application method will also direct our further research on the fate and transport of the applied NPs in the environment.

5. Conclusion

The direct application of MONPs by mixing them with CM has resulted in 53.02–62.07% reductions of H_2S during the entire experimental period, and reductions of up to 83.82–98.10% from day 10. Additionally, the CH_4 yield was 1.213 times higher than that of the control.

Several conclusions are obtained from this study:

1. TiO_2 NPs are effective for enhancing methane generation in AD through EET, which can occur when anaerobic methanogenic Archaea are in contact with the nano-TiO_2. Furthermore, the TiO_2 effectively mitigates H_2S by absorbing SO_2/SO_3, forming irreversible Ti−S bonds.
2. The supplementation of biodigesters with Fe_2O_3 NPs improved anaerobic digestion, and consequently resulted in higher methane production and organic matter degradation through the release of $Fe^{+2/+3}$, which likely promoted the production of metabolic intermediates and activity of key enzymes in the methanogenic Archaea. Additionally, Fe_2O_3 NPs reduce the amount of H_2S in the digestate by forming a ferrous sulfide deposit (FeS).
3. The effectiveness of the MONPs for enhancing methane and biogas and mitigating the emission of hydrogen sulfide was dose-dependent.
4. The combination of 100 and 500 mg/L of Fe_2O_3 and TiO_2 NPs, respectively, may increase the rate of the aggregation and agglomeration, so their interactions with sulfur will decrease, allowing SRB to utilize more sulfate and release H_2S. In addition, the combination may result in a competing electron interaction between both metals that reduces their action on the sulfates.
5. TVFA and pH are two major components in AD and did not change significantly in this study. The higher acetic acid contents with higher methane emissions indicated that metal oxide NPs promote the emission of CH_4 through the reduction of H_2/CO_2 by hydrogen-utilizing methanogens.

Declaration of interest

None.

Acknowledgments

We extend our sincere thanks to the Egyptian Culture, Education and Science Bureau in Tokyo, Japan, and the Ministry of Higher Education and Scientific Research, Egypt for supporting this study.

References

Abdelsalam, E., Samer, M., Attia, Y., Abdel-Hadi, M., Hassan, H., Badr, Y., 2017. Influence of zero valent iron nanoparticles and magnetic iron oxide nanoparticles on biogas and methane production from anaerobic digestion of manure. Energy 120, 842–853. https://doi.org/10.1016/j.energy.2016.11.137.

Abdelsalam, E., Samer, M., Attia, Y.A., Abdel-Hadi, M.A., Hassan, H.E., Badr, Y., 2016. Comparison of nanoparticles effects on biogas and methane production from anaerobic digestion of cattle dung slurry. Renew. Energy 87, 592–598. https://doi.org/10.1016/j.renene.2015.10.053.

Adams, L.K., Lyon, D.Y., Alvarez, P.J., 2006. Comparative eco-toxicity of nanoscale TiO_2, SiO_2, and ZnO water suspensions. Water Res. 40, 3527–3532. https://doi.org/10.1016/j.watres.2006.08.004.

Ahring, B.K., 1995. Methanogenesis in thermophilic biogas reactors. Antonie Leeuwenhoek 67, 91–102.

Ambuchi, J.J., Zhang, Z., Shan, L., Liang, D., Zhang, P., Feng, Y., 2017. Response of anaerobic granular sludge to iron oxide nanoparticles and multi-wall carbon nanotubes during beet sugar industrial wastewater treatment. Water Res. 117, 87–94. https://doi.org/10.1016/j.watres.2017.03.050.

Andriamanohiarisoamanana, F.J., Matsunami, N., Yamashiro, T., Iwasaki, M., Ihara, I., Umetsu, K., 2017a. High-solids anaerobic mono-digestion of riverbank grass under thermophilic conditions. J. Environ. Sci. 52, 29–38. https://doi.org/10.1016/j.jes.2016.05.005.

Andriamanohiarisoamanana, F.J., Sakamoto, Y., Yamashiro, T., Yasui, S., Iwasaki, M., Ihara, I., Nishida, T., Umetsu, K., 2017b. The seasonal effects of manure management and feeding strategies on hydrogen sulphide emissions from stored dairy manure. J. Mater. Cycles Waste Manag. 19, 1253–1260. https://doi.org/10.1007/s10163-016-0519-7.

Andriamanohiarisoamanana, F.J., Sakamoto, Y., Yamashiro, T., Yasui, S., Iwasaki, M., Ihara, I., Tsuji, O., Umetsu, K., 2015. Effects of handling parameters on hydrogen sulfide emission from stored dairy manure. J. Environ. Manag. 154, 110–116. https://doi.org/10.1016/j.jenvman.2015.02.003.

Andriamanohiarisoamanana, F.J., Shirai, T., Yamashiro, T., Yasui, S., Iwasaki, M., Ihara, I., Nishida, T., Tangtaweewipat, S., Umetsu, K., 2018. Valorizing waste iron powder in biogas production: hydrogen sulfide control and process performances. J. Environ. Manag. 208, 134–141. https://doi.org/10.1016/j.jenvman.2017.12.012.

APHA, 2005. American Public Health Association. Standard Methods for the Examination of Water and Wastewater, twenty-first ed. American Public Health Association, Washington DC, pp. 1220p.

Bajpai, P., 2017. Basics of Anaerobic Digestion Process, Anaerobic Technology in Pulp and Paper Industry. Springer, pp. 7–12. https://doi.org/10.1007/978-981-10-4130-3.

Bioenergy, I., 1999. Biogas upgrading and utilisation. Task 24, 6475–6481.

Blazy, V., De Guardia, A., Benoist, J., Daumoin, M., Lemasle, M., Wolbert, D., Barrington, S., 2014. Odorous gaseous emissions as influence by process condition for the forced aeration composting of pig slaughterhouse sludge. Waste Manag. 34, 1125–1138. https://doi.org/10.1016/j.wasman.2014.03.012.

Casals, E., Barrena, R., Garcia, A., Gonzalez, E., Delgado, L., Busquets-Fite, M., Font, X., Arbiol, J., Glatzel, P., Kvashnina, K., Sanchez, A., Puntes, V., 2014. Programmed iron oxide nanoparticles disintegration in anaerobic digesters boosts biogas production. Small 10, 2801–2808. 2741. https://doi.org/10.1002/smll.201303703.

Casals, E., Gonzalez, E., Puntes, V.F., 2012. Reactivity of inorganic nanoparticles in

biological environments: insights into nanotoxicity mechanisms. J. Phys. D Appl. Phys. 45, 443001. https://doi.org/10.1088/0022-3727/45/44/443001.
Cervantes-Aviles, P., Ida, J., Toda, T., Cuevas-Rodriguez, G., 2018. Effects and fate of TiO_2 nanoparticles in the anaerobic treatment of wastewater and waste sludge. J. Environ. Manag. 222, 227–233. https://doi.org/10.1016/j.jenvman.2018.05.074.
Charles, W., Cord-Ruwisch, R., Ho, G., Costa, M., Spencer, P., 2006. Solutions to a combined problem of excessive hydrogen sulfide in biogas and struvite scaling. Water Sci. Technol. 53, 203–211.
Chen, Y., Mu, H., Zheng, X., 2014. Chronic response of waste activated sludge fermentation to titanium dioxide nanoparticles. Chin. J. Chem. Eng. 22, 1162–1167. https://doi.org/10.1016/j.cjche.2014.09.007.
Future-markets, 2011. The World Market for Nanoparticle Titanium Dioxide, vols. 1–67 Future markets, Inc., Edinburgh, Scotland, UK.
Garcia, A., Delgado, L., Tora, J.A., Casals, E., Gonzalez, E., Puntes, V., Font, X., Carrera, J., Sanchez, A., 2012. Effect of cerium dioxide, titanium dioxide, silver, and gold nanoparticles on the activity of microbial communities intended in wastewater treatment. J. Hazard Mater. 199–200, 64–72. https://doi.org/10.1016/j.jhazmat.2011.10.057.
Gonzalez-Estrella, J., Sierra-Alvarez, R., Field, J.A., 2013. Toxicity assessment of inorganic nanoparticles to acetoclastic and hydrogenotrophic methanogenic activity in anaerobic granular sludge. J. Hazard Mater. 260, 278–285. https://doi.org/10.1016/j.jhazmat.2013.05.029.
Kadam, R., Panwar, N., 2017. Recent advancement in biogas enrichment and its applications. Renew. Sustain. Energy Rev. 73, 892–903. https://doi.org/10.1016/j.rser.2017.01.167.
Kim, J.Y., Park, H.-J., Lee, C., Nelson, K.L., Sedlak, D.L., Yoon, J., 2010. Inactivation of Escherichia coli by nanoparticulate zerovalent iron and ferrous ion. Appl. Environ. Microbiol. 76, 7668–7670. https://doi.org/10.1128/AEM.01009-10.
Kubo, M., Onodera, R., Shibasaki-Kitakawa, N., Tsumoto, K., Yonemoto, T., 2005. Kinetics of ultrasonic disinfection of Escherichia coli in the presence of titanium dioxide particles. Biotechnol. Prog. 21, 897–901. https://doi.org/10.1021/bp049729s.
Kumar, N., Omoregie, E.O., Rose, J., Masion, A., Lloyd, J.R., Diels, L., Bastiaens, L., 2014. Inhibition of sulfate reducing bacteria in aquifer sediment by iron nanoparticles. Water Res. 51, 64–72. https://doi.org/10.1016/j.watres.2013.09.042.
Lateef, S.A., Beneragama, N., Yamashiro, T., Iwasaki, M., Umetsu, K., 2014. Batch anaerobic co-digestion of cow manure and waste milk in two-stage process for hydrogen and methane productions. Bioproc. Biosyst. Eng. 37, 355–363. https://doi.org/10.1007/s00449-013-1000-9.
Li, H., Cui, F., Liu, Z., Li, D., 2017. Transport, fate, and long-term impacts of metal oxide nanoparticles on the stability of an anaerobic methanogenic system with anaerobic granular sludge. Bioresour. Technol. 234, 448–455. https://doi.org/10.1016/j.biortech.2017.03.027.
Liu, C., Yuan, H., Zou, D., Liu, Y., Zhu, B., Li, X., 2015. Improving biomethane production and mass bioconversion of corn stover anaerobic digestion by adding NaOH pretreatment and trace elements. BioMed Res. Int 2015. https://doi.org/10.1155/2015/125241.
Liu, R., Lal, R., 2015. Potentials of engineered nanoparticles as fertilizers for increasing agronomic productions. Sci. Total Environ. 514, 131–139. https://doi.org/10.1016/j.scitotenv.2015.01.104.
Lupitskyy, R., Alvarez-Fonseca, D., Herde, Z.D., Satyavolu, J., 2018. In-situ prevention of hydrogen sulfide formation during anaerobic digestion using zinc oxide nanowires. J. Environ. Chem. Eng. 6, 110–118. https://doi.org/10.1016/j.jece.2017.11.048.
Lyu, S., Wei, X., Chen, J., Wang, C., Wang, X., Pan, D., 2017. Titanium as a beneficial element for crop production. Front. Plant Sci. 8, 597. https://doi.org/10.3389/fpls.2017.00597.
Marsalek, B., Jancula, D., Marsalkova, E., Mashlan, M., Safarova, K., Tucek, J., Zboril, R., 2012. Multimodal action and selective toxicity of zerovalent iron nanoparticles against cyanobacteria. Environ. Sci. Technol. 46, 2316–2323. https://doi.org/10.1021/es2031483.
Mu, H., Chen, Y., 2011. Long-term effect of ZnO nanoparticles on waste activated sludge anaerobic digestion. Water Res. 45, 5612–5620. https://doi.org/10.1016/j.watres.2011.08.022.
Mu, H., Chen, Y., Xiao, N., 2011. Effects of metal oxide nanoparticles (TiO_2, Al_2O_3, SiO_2 and ZnO) on waste activated sludge anaerobic digestion. Bioresour. Technol. 102, 10305–10311. https://doi.org/10.1016/j.biortech.2011.08.100.
Muñoz, R., Meier, L., Diaz, I., Jeison, D., 2015. A review on the state-of-the-art of physical/chemical and biological technologies for biogas upgrading. Rev. Environ. Sci. Biotechnol. 14, 727–759. https://doi.org/10.1007/s11157-015-9379-1.
Muyzer, G., Stams, A.J., 2008. The ecology and biotechnology of sulphate-reducing bacteria. Nat. Rev. Microbiol. 6, 441. https://doi.org/10.1038/nrmicro1892.
Nel, A., Xia, T., Mädler, L., Li, N., 2006. Toxic potential of materials at the nanolevel. Science 311, 622–627. https://doi.org/10.1126/science.1114397.
Noonari, A., Mahar, R., Sahito, A., Brohi, K., 2018. Anaerobic Co-digestion of canola straw and banana plant wastes with buffalo dung: effect of Fe_3O_4 nanoparticles on methane yield. Renew. Energy. https://doi.org/10.1016/j.renene.2018.10.113.
Pipatmanomai, S., Kaewluan, S., Vitidsant, T., 2009. Economic assessment of biogas-to-electricity generation system with H_2S removal by activated carbon in small pig farm. Appl. Energy 86, 669–674. https://doi.org/10.1016/j.apenergy.2008.07.007.
Qiang, H., Niu, Q., Chi, Y., Li, Y., 2013. Trace metals requirements for continuous thermophilic methane fermentation of high-solid food waste. Chem. Eng. J. 222, 330–336. https://doi.org/10.1016/j.cej.2013.02.076.
Rincón, A., Pulgarin, C., 2003. Photocatalytical inactivation of E. coli: effect of (continuous–intermittent) light intensity and of (suspended–fixed) TiO_2 concentration. Appl. Catal. B Environ. 44, 263–284. https://doi.org/10.1016/S0926-3373(03)00076-6.
Sarker, N.C., Rahman, S., Borhan, M.S., Rajasekaran, P., Santra, S., Ozcan, A., 2018. Nanoparticles in mitigating gaseous emissions from liquid dairy manure stored under anaerobic condition. J. Environ. Sci. 76, 26–36. https://doi.org/10.1016/j.jes.2018.03.014.
Ševců, A., El-Temsah, Y.S., Joner, E.J., Černík, M., 2011. Oxidative stress induced in microorganisms by zero-valent iron nanoparticles. Microb. Environ. 26, 271–281. https://doi.org/10.1264/jsme2.ME11126.
Skocaj, M., Filipic, M., Petkovic, J., Novak, S., 2011. Titanium dioxide in our everyday life; is it safe? Radiol. Oncol. 45, 227–247.
Su, L., Shi, X., Guo, G., Zhao, A., Zhao, Y., 2013. Stabilization of sewage sludge in the presence of nanoscale zero-valent iron (nZVI): abatement of odor and improvement of biogas production. J. Mater. Cycles Waste Manag. 15, 461–468. https://doi.org/10.1007/s10163-013-0150-9.
Sun, C., Lee, J.S., Zhang, M., 2008. Magnetic nanoparticles in MR imaging and drug delivery. Adv. Drug Deliv. Rev. 60, 1252–1265. https://doi.org/10.1016/j.addr.2008.03.018.
Wang, C.-T., Ro, S.-H., 2007. Nanoparticle iron–titanium oxide aerogels. Mater. Chem. Phys. 101, 41–48. https://doi.org/10.1016/j.matchemphys.2006.02.010.
Wang, G., Feng, H., Gao, A., Hao, Q., Jin, W., Peng, X., Li, W., Wu, G., Chu, P.K., 2016a. Extracellular electron transfer from aerobic bacteria to Au-loaded TiO_2 semiconductor without light: a new bacteria-killing mechanism other than localized surface plasmon resonance or microbial fuel cells. ACS Appl. Mater. Interfaces 8, 24509–24516. https://doi.org/10.1021/acsami.6b10052.
Wang, T., Zhang, D., Dai, L., Chen, Y., Dai, X., 2016b. Effects of metal nanoparticles on methane production from waste-activated sludge and microorganism community shift in anaerobic granular sludge. Sci. Rep. 6, 25857. https://doi.org/10.1038/srep25857.
Yang, Y., Zhang, C., Hu, Z., 2013. Impact of metallic and metal oxide nanoparticles on wastewater treatment and anaerobic digestion. Environ. Sci.: Process. Impact. 15, 39–48. https://doi.org/10.1039/C2EM30655G.
Yanxin, C., Yi, J., Wenzhao, L., Rongchao, J., Shaozhen, T., Wenbin, H., 1999. Adsorption and interaction of H_2S/SO_2 on TiO_2. Catal. Today 50, 39–47. https://doi.org/10.1016/S0920-5861(98)00460-X.
Zhang, L., Jahng, D., 2012. Long-term anaerobic digestion of food waste stabilized by trace elements. Waste Manag. 32, 1509–1515. https://doi.org/10.1016/j.wasman.2012.03.015.
Zhang, L., Loh, K.-C., Zhang, J., 2018. Enhanced biogas production from anaerobic digestion of solid organic wastes: current status and prospects. Bioresour. Technol. Rep. https://doi.org/10.1016/j.biteb.2018.07.005.
Zhang, W., Wei, Q., Wu, S., Qi, D., Li, W., Zuo, Z., Dong, R., 2014a. Batch anaerobic co-digestion of pig manure with dewatered sewage sludge under mesophilic conditions. Appl. Energy 128, 175–183. https://doi.org/10.1016/j.apenergy.2014.04.071.
Zhang, Y., Feng, Y., Yu, Q., Xu, Z., Quan, X., 2014b. Enhanced high-solids anaerobic digestion of waste activated sludge by the addition of scrap iron. Bioresour. Technol. 159, 297–304. https://doi.org/10.1016/j.biortech.2014.02.114.
Zhou, Q., Jiang, X., Li, X., Jiang, W., 2016. The control of H_2S in biogas using iron ores as in situ desulfurizers during anaerobic digestion process. Appl. Microbiol. Biotechnol. 100, 8179–8189. https://doi.org/10.1007/s00253-016-7612-7.